The *fasciated ear2* gene encodes a leucine-rich repeat receptor-like protein that regulates shoot meristem proliferation in maize

Fumio Taguchi-Shiobara,[1] Zhuang Yuan, Sarah Hake,[2] and David Jackson[3]

Cold Spring Harbor Laboratory, Cold Spring Harbor, New York 11724, USA

The ability to initiate organs throughout the lifecycle is a unique feature of plant development that is executed by groups of stem cells called meristems. The balance between stem cell proliferation and organ initiation is carefully regulated and ensures that organs can be initiated in regular geometric patterns. To understand how this regulation is achieved, we isolated a novel mutant of maize, *fasciated ear2* (*fea2*), which causes a massive overproliferation of the ear inflorescence meristem and a more modest effect on floral meristem size and organ number. We cloned the *fea2* gene using transposon tagging, and it encodes a membrane localized leucine-rich repeat receptor-like protein that is most closely related to *CLAVATA2* from *Arabidopsis*. These findings provide evidence that the *CLAVATA* pathway for regulation of meristem size is functionally conserved throughout the angiosperms. A possible connection of *fea2* to the control of crop yields is discussed.

Plant development is highly dynamic and involves the reiterative initiation of new primordia from groups of stem cells called meristems. Leaves and the axillary meristems that generate branches and flowers are initiated in regular patterns from the shoot apical meristem (SAM). SAMs have a remarkable ability to regulate their size during development, by exquisitely balancing cell proliferation with the incorporation of cells into new primordia (Sussex 1952; Medford 1992; Weigel and Clark 1996; Meyerowitz 1997). This balance is essential to maintain SAM integrity and the stereotypical pattern of organ initiation throughout development. Therefore, understanding the mechanisms regulating stem cell fate and proliferation is key to understanding SAM function and patterning of the shoot.

Genetic analysis of shoot meristem biology has progressed significantly in recent years (Evans and Barton 1997; Laufs et al. 1998b; Bowman and Eshed 2000). Mutants affecting meristem size can be grouped into two classes. The first class includes those affecting meristem formation and maintenance. For example, in strong alleles of *shootmeristemless* (*stm*), seedlings arrest with no obvious shoot meristem after forming the cotyledons (Barton and Poethig 1993), though weak alleles indicate a role for *STM* throughout all stages of shoot development (Clark et al. 1996; Endrizzi et al. 1996). *STM* encodes a *knotted1* (*kn1*)-related homeodomain protein, and consistent with their role in SAM initiation and maintenance, these genes are expressed throughout the SAM and down-regulated on the flanks where organs are initiated (Smith et al. 1992; Jackson et al. 1994; Long et al. 1996; Kerstetter et al. 1997; Vollbrecht et al. 2000). *wuschel* (*wus*) mutants are also impaired in stem cell maintenance (Laux et al. 1996). *WUS* encodes a homeodomain protein that is expressed before SAM initiation in the embryo, and becomes localized to a group of cells that underlies the presumptive stem cells, suggesting that it may signal stem cell fate nonautonomously (Mayer et al. 1998).

A second class of SAM mutants causes meristem enlargement, which in extreme cases can lead to fasciation. The term fasciation, from the Latin *fascis*, meaning bundle, describes variations in plant form resulting from proliferative growth. Fasciation was one of Mendel's 14 heritable characters in pea, and also has a long history of study in maize (Emerson 1912). Fasciated variants have significantly increased crop yields, for instance by increasing fruit size in tomato (Luckwill 1943; Zielinski 1945).

Mutations in *Arabidopsis* that cause meristem enlargement include the *clavata* (*clv*) mutations (Leyser and Furner 1992; Clark et al. 1993, 1995; Kayes and Clark 1998), *mgoun1* and *mgoun2* (Laufs et al. 1998a), *fasciata1* and *fasciata2* (Leyser and Furner 1992; Kaya et al. 2001), and *fully fasciated* (Medford et al. 1992). *clv* mutants have larger shoot meristems and increased floral organ number, and strong alleles of *clv1* and *clv3* often fasciate (Clark et al. 1993, 1995). In contrast, *clv2* mutants have relatively weak phenotypes, similar to weak *clv1* or *clv3* alleles; fasciation in *clv2* mutants is observed only rarely, and only under short day growth conditions, possibly indicating genetic redundancy (Kayes and Clark 1998). *clv3* mutants dominantly enhance *clv1* (Clark et al. 1995), and *clv2* mutants enhance weak or intermediate alleles of *clv1* or *clv3* (Kayes and Clark 1998), suggesting that these three genes act in the same pathway to regulate shoot meristem size. Insight into the molecular nature of this pathway has come from isolation of the *CLV* genes; *CLV1* encodes a transmembrane leucine-rich repeat (LRR)-kinase, *CLV2* encodes a protein with predicted transmembrane and LRR domains and only a very short intracellular region, and *CLV3* encodes a small protein that is predicted to be secreted (Clark et al. 1997; Fletcher et al. 1999; Jeong et al. 1999). Mosaic analysis of *CLV3* supports the hypothesis that it encodes an intercellular signaling molecule (Fletcher et al. 1999). Biochemical studies have shown that CLV1 is present in two complexes; the smaller one consists of a disulfide-linked multimer, and the larger complex contains CLV3, the KAPP phosphatase, and a Rho-related GTPase, both possible downstream effectors. CLV1 and CLV3 are required for formation of the large complex (Trotochaud et al. 1999, 2000). The precise role of CLV2 in this pathway is unclear, although the observations that the accumulation of CLV1 protein is severely reduced in *clv2* mutants (Kayes and Clark 1998; Jeong et al. 1999), and that CLV3 binds to yeast cells expressing CLV1 and CLV2 (Trotochaud et al. 2000) suggest that CLV1 and CLV2 proteins act as a heterodimer receptor complex. Some of these predictions are supported by *CLV3* overexpression studies (Brand et al. 2000).

Despite these significant insights into meristem function in *Arabidopsis*, little is known about whether the mechanisms are conserved in other species. In particular, fasciated mutants have not been characterized at a molecular level in other plants. Interspecific differences in SAM structure and function make it interesting to ask how well conserved are the genes that control meristem development in *Arabidopsis*. Developmental changes in meristem function may underlie the yield increases brought about during the domestication and breeding of crops, and so it would be particularly interesting to understand how these genes function in crop plants. Maize is a good model system for cereal crop genetics and development, because of its rich genetic heritage and well-characterized morphology (Poethig 1993).

The maize ear is a particularly interesting system, as its development involves several meristem identity decisions (for review, see McSteen et al. 2000). The ear inflorescence meristem forms several rows of secondary meristems called spikelet pair meristems in a regular polystichous phyllotaxy. These meristems branch to form a pair of spikelet meristems, which branch again, to generate a pair of floral meristems. In the ear, one of the flowers will abort, and the other, when pollinated, will generate a single seed. The cob structure of the maize ear is unique among the grasses (Kellogg and Birchler 1993), and is evolutionarily derived from the distichous inflorescence of teosinte (Beadle 1980; Doebley 1992). However, teosinte inflorescences produce only a single alternating row of seeds, whereas modern maize lines produce from 8 to 18, and some varieties up to 36 rows of seeds (USDA, ARS, National Genetic Resources Program, Germplasm Resources Information Network; http://www.ars-grin.gov/cgi-bin/npgs/). The ability of the inflorescence meristem to initiate a larger number of the secondary meristems that generate seed rows appears to be a major factor in the development of maize as a crop plant, and it would therefore be interesting to understand the mechanisms that regulate this aspect of ear inflorescence meristem function.

Here we describe a novel mutant of maize, *fasciated ear2* (*fea2*). *fea2* plants develop larger meristems during inflorescence and floral shoot development, and ear inflorescence meristems show severe fasciation, suggesting that *fea2* normally acts to limit the growth of these meristems. *fea2* encodes an LRR protein that is targeted to the plasmamembrane, suggesting that it acts as a receptor. *fea2* is most closely related to the *CLV2* gene of *Arabidopsis*, suggesting that the *CLAVATA* pathway is functionally conserved in monocot species.

Results

Phenotypic analysis of fea2 mutants

The original *fea2* allele, *fea2-0*, arose in a nontargeted screen of *Mutator* transposon families. A single family segregated plants with abnormally flattened ears, and sib and out crosses together with subsequent introgressions indicated that the mutation segregated as a simple recessive trait. A similar mutation was previously identified and named *fasciated ear* (Hake and Veit 1988). The new mutation was not allelic to *fasciated ear*, and we therefore named it *fasciated ear2* (*fea2*). We have introgressed *fea2* into several genetic backgrounds, and it shows strong phenotypic expression in all of them; we will describe the phenotypes of *fea2* in the B73 genetic background. Unlike some *Mu* induced alleles (Martienssen and Baron 1994), there was no effect of *Mu* activity on the expressivity of the *fea2* phenotype (data not shown).

Maize plants generate two distinct inflorescence structures; the terminal tassel bears male flowers, whereas the lateral inflorescences, the ears, bear female flowers. The most obvious phenotype of *fea2* plants was in the development of the ears, which at maturity were abnormally flattened and wider than normal, with irregular rows of seeds (Fig. 1). The seed rows were irregular even

Figure 1. Mature ear and tassel phenotypes. From left, normal inbred B73 ear (female inflorescence), showing straight vertical rows of kernels. Next, an *fea2* ear is shorter and wider than normal and is flattened, and the rows of kernels are irregular. The *fea2* ear contains more vertical rows of kernels. Next, normal and *fea2* tassel (male inflorescence) at this magnification appear similar. To the right, a higher magnification of part of the central spike of normal and *fea2* tassels, from which some of the spikelets have been stripped in the central region. Note that the rachis or stem of the *fea2* tassel spike is thicker than that of the normal tassel.

at the base of the ear, indicating that ear development was perturbed from an early stage. *fea2* ears can have up to double the normal number of vertical rows of seeds (Table 1). However, as they are also shorter than normal the overall seed yield may not be higher. Compared to the ear, the tassel of *fea2* plants was relatively normal, but when the spikelets were stripped off the central spike it was obvious that the rachis was slightly wider than normal, though it was not flattened or fasciated (Fig. 1). Consistent with the thicker rachis of *fea2* tassels, the spikelet density in the tassel central spike was higher than normal (Table 1).

To determine when *fea2* first affects meristem development, we measured shoot meristem size in cleared tissue slices. During vegetative seedling development, *fea2* shoot meristems were almost indistinguishable from their normal sibs; meristem width was the same as normal and meristem height was slightly greater in *fea2*,

Table 1. *Meristem size and inflorescence characteristics in normal and* fea2 *ears*

| | Vegetative SAM size[a] | | Seed row no. in ear[b] | Spikelet density in tassel[c] |
	width/μm	height/μm		
B73	139 (16)	135 (19)	16–18	5.8 (0.3)
fea2	137 (8)	150 (17)	26–36	6.8 (0.8)

Numbers are mean values, with standard deviation in parentheses, except for row number, which shows the range of values.
[a]Measurements made on 14-day-old seedlings having ~5 visible leaves, n = 6–12.
[b]Range of number of vertical rows of seed in mid point of ear; n = 10.
[c]Number of spikelet pairs per cm on central spike of mature tassel, >300 spikelets were counted on 6–10 different tassels. Values for *fea2* and B73 are significantly different by *t*-test ($P < 0.05$).

though this may not be statistically significant (Table 1). In accord with these observations, *fea2* plants showed no obvious abnormalities during vegetative development (data not shown). The ears are produced from lateral shoots, which first undergo a vegetative phase of development and produce several husk leaves before undergoing the transition to inflorescence development. During this transition, which under our growth conditions occurred between 25 and 30 days after planting, the size of the lateral shoot meristems increased slightly in normal B73 plants (Fig. 2). *fea2* lateral ear shoot meristems were slightly wider and about twice as tall as normal prior to the inflorescence transition. However, around the time of this transition they enlarged profoundly, and almost doubled in both height and width in a few days (Fig. 2). Therefore, *fea2* acts to restrict lateral meristem size even before the inflorescence transition, but it is around the time of the transition that the *fea2* mutant phenotype starts to be especially pronounced.

To visualize changes in inflorescence morphology, we observed immature ears during development using a scanning electron microscope. When *fea2* ears were only 1–2 mm in length, the inflorescence meristem was obviously fasciated (Fig. 3C). Sections through ears at this stage hybridized in situ with *knotted1* (*kn1*), a shoot meristem marker gene, showed that the whole of the fasci-
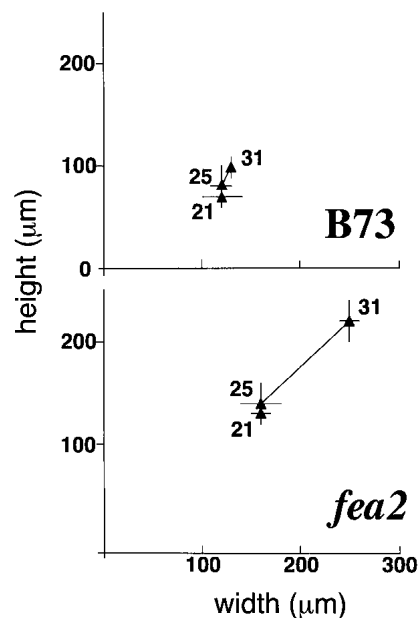

Figure 2. Meristem sizes in normal and *fea2* lateral ear shoots. *fea2* meristems proliferate significantly at the time of the inflorescence transition. The graph shows changes in the mean lateral shoot meristem width and height, measured immediately distal to the most recently initiated primordium, at 21, 25, and 31 d after planting. Measurements were taken from the uppermost lateral ear shoot from each plant; for each sample, n = 3–6. Vertical and horizontal lines show standard deviation in height and width measurements, respectively. Note that the transition from vegetative to inflorescence development occurred between 25 and 31 d in these samples.
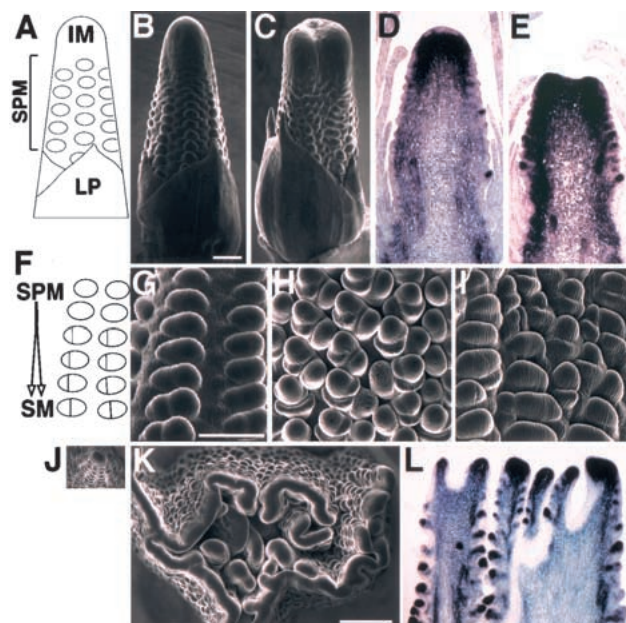
Figure 3. Morphogenesis and gene expression in normal and *fea2* ears. (*A*) Schematic of an ear primordium showing inflorescence meristem (IM), spikelet pair meristems (SPM), and some of the surrounding husk leaf primordia (LP). (*B*) A normal, B73 inbred ear primordium. Bar, 250 μm. (*C*) An *fea2* ear primordium at a similar developmental stage. The tip of this ear primordium is flattened and a furrow is starting to form, and the rows of SPMs are irregular. (*D,E*) Sections through similar stage of normal and *fea2* ear primordia, respectively, probed in situ for *kn1* mRNA. Both samples show strong staining at the tip of the ear shoot and sporadic staining on the sides when the section passes through an SPM. As ear development progresses, SPMs on the flank of the ear shoot branch to generate a pair of spikelet meristems (SMs), shown schematically in (*F*). In normal ears (*G*), this occurs as a gradual progression and generates pairs of spikelets that remain aligned in vertical rows. Bar, 250 μm. In *fea2* ears, the plane of SPM branching and extent of branching is irregular *H,I*. In *H*, some SPMs appear to branch more than once, whereas in (*I*), branching appears to be delayed, and wide, flattened SPMs are visible. At a later stage of development (*J–L*), when the ear primordia are around 1 cm long, the *fea2* ear inflorescence phenotype is much more severe. SEM views looking down on the inflorescence meristem of a normal ear (*J*) and *fea2* ear (*K*) are shown at the same magnification. Bar in *K*, 1000 μm. In *L*, a section through an *fea2* ear at a similar stage to the one shown in *K*, probed in situ for *kn1*, shows strong *kn1* expression at the tips of each branch.

ated apical region expressed *kn1* strongly, indicating that it had normal shoot meristem identity.

We also observed abnormal development of the other meristem types on *fea2* ears. The inflorescence meristem normally initiates spikelet pair meristems (SPMs) in a regular phyllotaxy, and the SPMs later branch to generate a pair of spikelet meristems (SMs) that are aligned in adjacent vertical rows (Fig. 3F,G). In *fea2* ears, both the timing and orientation of SPM branching was disrupted, giving rise to irregular clusters of SMs as well as enlarged and flattened SPMs (Fig. 3H,I). As development proceeded, the fasciation became progressively

more severe, and the apical region of *fea2* ears enlarged to be more than 20 times wider than normal when the ears were 1–2 cm in length (Fig. 3, normal ear, J, shown at same magnification as *fea2* ear, K). The *fea2* inflorescence meristem spread out into a ring and also split to generate many smaller inflorescence-like structures which also expressed *kn1* strongly at their tips, suggesting that they retained shoot meristem identity (Fig. 3L). Consistent with the relatively mild phenotypes in the tassel, the tassel inflorescence meristems did not massively overproliferate, and were only mildly enlarged or fasciated (not shown).

Later in inflorescence development, each spikelet meristem branches to form a pair of floral meristems. In the ear, one of the floral meristems aborts, so only a single flower develops in each spikelet. On normal ears, the spikelets are paired (Fig. 4A,D); in *fea2* ears, spikelets were occasionally in clusters of three (Fig. 4B), presumably as a consequence of the abnormal enlargement and branching of the SPMs observed at an earlier stage of development. Flower development was also abnormal in *fea2* ears. Usually the floral meristem terminates with the production of the gynoecium, which contains three carpels, two of which grow out and fuse to form the forked silk (Fig. 4D). In *fea2* ears, the gynoecium was often enlarged, and around 46% of the flowers ($n = 100$) produced extra carpel-like structures that were often fused (Fig. 4E).

fea2 mutants also developed abnormal spikelets and flowers in the tassel. One of the spikelets in the spikelet pair is supported on an extended internode called a pedicel (arrowed in Fig. 4F). *fea2* spikelet pairs had consistently longer pedicels (Fig. 4H); the mean pedicel length in *fea2* spikelet pairs was 6.9 ± 1.7 mm, compared to normal pedicels, which were 5.1 ± 1.4 mm ($n = 50$). In addition, *fea2* flowers had an abnormal numbers of stamens; male spikelets normally contain two flowers, each of which have three stamens (Fig. 4G). *fea2* flowers had irregular numbers of stamens in 48% of their flowers ($n = 50$); the majority of abnormal flowers contained four stamens (Fig. 4I, arrowed).

To summarize, *fea2* plants were defective in the regulation of meristem size in lateral branch and inflorescence phases, and the phenotype was most striking in the female inflorescence meristem. *fea2* flowers produced extra carpel-like structures in the ear and extra stamens in the tassel. Therefore, in the normal inflorescence shoot, *fea2* acts to limit the growth of all meristem types.

Isolation of the fea2 gene

Southern analysis using probes specific for different classes of *Mu* transposons identified a 4 kb *Mu8* hybridizing *Sst*I fragment that cosegregated with *fea2-0* in ~80 individuals and was not present in sibling families that did not carry the *fea2* mutation (data not shown). We used introgressed families that were selected for loss of *Mu* activity and contained many fewer *Mu* hybridizing bands to identify a larger cosegregating fragment, a 16 kb
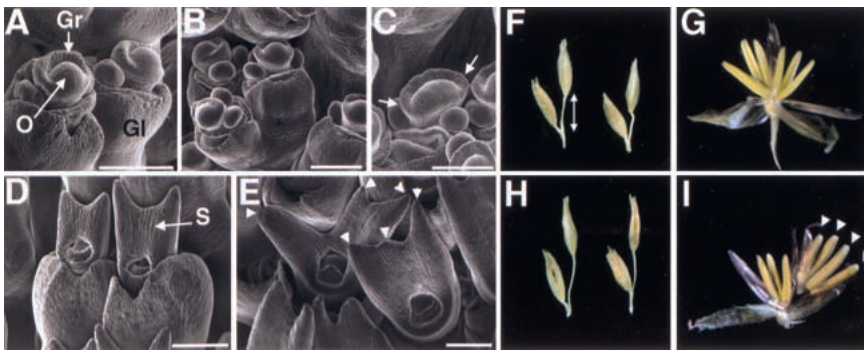
Figure 4. Abnormal spikelet and floral development in *fea2* ears. Normal ears have spikelets arranged in pairs, each subtended by a leaf-like organ, the glume (Gl) (*A,D*), and in each spikelet a single flower develops. The ovule primordium (O) and gynoecial ridge (Gr), formed by the fusion of two carpel primordia, are visible in *A*. In *D*, at a later stage of development, the gynoecial ridge of each flower has grown out to form the forked silk primordium (S), which is starting to cover the ovule primordium. *fea2* ear spikelets and flowers are shown in *B*, *C*, and *E*. An abnormal clustering of three spikelets is seen in *B*. In *C*, the ovule primordium is enlarged and surrounded by a wider gynoecial ridge (arrowed). Two flowers with irregular numbers of carpels (arrowed) contributing to the silks are shown in *E*. Bar in each panel, 250 μm. *fea2* plants also show defects in spikelet and flower development in the tassel. Normal male spikelets are arranged in pairs, and one is supported on an extended internode called a pedicel (arrow, *F*). The pedicels in *fea2* (*H*) are longer than normal; representative spikelets from the base (*left*) and middle region (*right*) of the tassel central spike are shown. In the tassels, spikelets normally contain two flowers, each with three anthers (*G*); in the *fea2* spikelet (*I*), one of the flowers frequently contains four anthers (arrowed).

*Bam*HI fragment that encompassed the 4 kb *Sst*I fragment. Size-fractionated *Bam*HI-digested genomic DNA from *fea2-0* plants was cloned into a lambda phage library, and the library was probed with a *Mu8* probe. Four positive clones were purified and restriction mapped, and subclones were isolated for analysis. One subclone, corresponding to the 550 bp to the right side of the *Mu8* element, identified a polymorphism between *fea2-0* individuals and normal sibs (Fig. 5A). In *Sst*I-digested *fea2-0* genomic DNA, the 550-bp probe detected a single band of 4 kb, as expected, and a smaller band of around 2.5 kb in normal sibs; the size difference corresponds to the size of the *Mu8* transposon.

To determine whether the cloned fragment corresponded to *fea2*, we isolated a new *fea2* allele by directed *Mu* transposon tagging. *fea2-0* homozygotes were crossed onto *Mu* active plants, and 30,000 F_1 seeds were planted in the 1999 summer field. Ears were screened at the time of pollen shed for fasciation. A single plant with severely fasciated ears was found in family 846. This plant was out-crossed to *fea2-0* and to normal testers, and analysis of F_1 and F_2 generations confirmed that the new allele, designated *fea2-846*, was allelic to *fea2-0* and when homozygous had a phenotype indistinguishable from that of *fea2-0* (data not shown). Southern analysis using the 550-bp flanking probe identified a novel polymorphism of 3 kb in size associated with this allele (Fig. 5A), confirming that we had correctly isolated the *fea2* gene. Sequencing of this allele revealed that it was caused by the insertion of a *Mu7* transposable element ~300 bp downstream of the position of the *Mu8* insertion in *fea2-0* (Fig. 5C). We mapped *fea2* using recombinant inbred lines (Burr et al. 1988) to chromosome 4, bin 05, between markers uaz265c and npi284.

fea2 *is expressed widely in the shoot*

To identify an *fea2* transcript, we probed RNA gel blots with the 550-bp probe. A single transcript of ~2.5 kb was detected in total RNA isolated from ear primordia, vegetative apex, and young leaf tissues, consisting of primordia still wrapped up in the whorl (Fig. 6). A very weak signal was detected in expanded leaf tissues, and no transcript was detected in root tissues. *fea2* transcript was not found in extracts from *fea2-0* mutant ear primordia, and a control probing with *kn1* confirmed the integrity of these RNA extracts. Two ESTs for *fea2* were recently sequenced from a 1–3 mm tassel cDNA library (http://gremlin3.zool.iastate.edu/zmdb/EST/). Therefore, *fea2* is expressed in immature ear, tassel, vegetative apex, and young leaf tissues, and the transcript is not detected in *fea2* ears. Despite several attempts using probes from different regions of the cDNA, we have been unable to detect a specific signal for *fea2* by in situ hybridization, and conclude that the transcript is likely expressed widely rather than being concentrated in a specific domain or region of the apical region.

The lack of *fea2* transcript in *fea2-0* ears, together with the position of the *Mu8* element in the exon, led us to suspect that *fea2-0* was a null allele. To test this hypothesis genetically, we made plants hemizygous for *fea2-0* using the TB 4Lc translocation stock (Birchler 1993). These plants developed ears with a fasciated phenotype similar to *fea2-0* homozygotes (data not shown). Although this analysis was performed in a mixed genetic background, our observations suggest that the *fea2-0* allele behaves genetically as a null (Muller 1932).

fea2 *encodes a predicted leucine-rich repeat receptor*

To identify the complete *fea2* transcript, we used a combination of 5′ and 3′ RACE PCR (Frohman et al. 1988), using primers designed against the 550-bp clone to amplify cDNA prepared from 5–10 mm ear primordia. The products were subcloned and sequenced, and the sequences assembled and translated in silico. The 3′ RACE product contained 421 bp downstream of the first in-frame stop codon in the major open reading frame. The
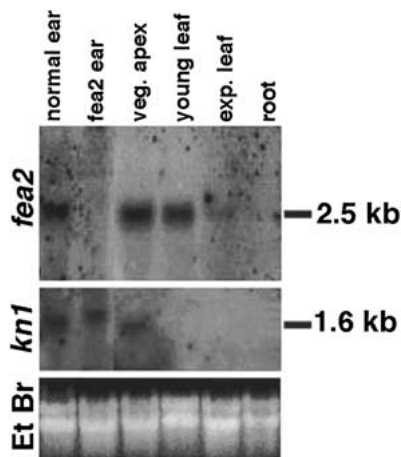
Figure 5. Molecular characterization of *fea2*. (*A*) Southern blot of *Sst*I-digested genomic DNA from (1) *fea2-0* homozygous mutant, (2) normal sib, (3) *fea2-0* heterozygote, and (4) *fea2-0/fea2-846* heterozygote. Note the novel 3 kb polymorphism in this plant associated with the *fea2-846* mutation. The probe was the 550-bp fragment downstream of the *Mu8* element in *fea2-0*. Values on the left side represent size in kb. (*B*) Schematic of predicted domains in FEA2 and CLV2 proteins. (*C*) CLUSTALW (http://dot.imgen.bcm.tmc.edu:9331/multialign/Help/clustalw.html) alignment of FEA2 (from B73 inbred line; top line) and CLV2 (below, Genbank accession no. AAF02655). Identical residues are outlined in black, similar in gray; dashes represent gaps introduced to optimize the alignment, and "empty" gaps are introduced to separate each LRR motif, according to Thomas et al. (1997). Arrows indicate positions of the *Mu* transposon insertions in the two *fea2* mutant alleles. Predictions of transmembrane and signal sequences are by SMART (http://smart.embl-heidelberg.de/) for FEA2 and from Jeong et al. (1999) for CLV2. These features are labeled above and below the respective sequences. (>>>) Signal peptide; (~~~) transmembrane domain; (* *) cysteine pair.

Figure 6. *fea2* expression analysis. Total RNA, 10 µg/lane from normal ear primordia, *fea2* ear primordia (5–15 mm long), vegetative seedling apex, young, unexpanded leaf, expanded leaf, and root tissues. *fea2* is expressed in normal ear primordia, vegetative apex, and young leaf tissue. Control probing with *kn1* shows a signal in normal ear, *fea2* ear, and vegetative apex, but not in leaf or root, as expected. Lower panel is the RNA gel stained with ethidium bromide and photographed on a UV light box, showing equal loading of RNA in all lanes.

longest 5′ RACE product contained 43 bp upstream of the first in frame ATG (data not shown). Comparison of the transcript sequence with that of the genomic DNA from the *Mu* flanking clone indicated that the predicted *fea2* coding sequence is encoded by a single large exon.

A BLASTP search using the predicted translation of *fea2* indicated similarity to a large number of plant receptor LRR proteins, with identity in the range of 30–34%; however, the similarity was restricted to the LRR regions (data not shown). Only a single protein, CLV2, had significantly greater similarity to FEA2 that also included the non-LRR regions (44% amino acid identity over most of the sequence, 58% similarity, Fig. 5C). Protein targeting and motif searching using SMART (http://smart.embl-heidelberg.de/) analysis predicted that FEA2

contains a signal peptide, a block of LRRs interrupted by a 40 amino acid island region, a transmembrane region and a 15 amino acid cytoplasmic tail (Fig. 5B). This domain structure is conserved in CLV2, except that CLV2 is predicted to have four more LRR repeats in the amino terminal cluster (Fig. 5B). A CLUSTALW alignment of FEA2 and CLV2 reveals that similarity is spread over the whole of the polypeptide sequence, although it is enhanced in the LRRs (Fig. 5C). For clarity, we introduced spaces in the alignments between each predicted LRR repeat, and it was clear that significant blocks of identity and similarity in the LRRs overlapped with the predicted solvent exposed residues thought to be involved in protein–ligand interaction (Kobe and Deisenhofer 1995; Thomas et al. 1997). In summary, FEA2 is closely related to the *Arabidopsis* CLV2 protein, and is predicted to contain extracytoplasmic LRRs, a transmembrane domain, and a short cytoplasmic tail.

FEA2–GFP localizes to the plasma membrane

To test the predicted membrane localization of FEA2, we made a translational fusion with a plant-optimized green fluorescent protein (GFP) (mGFP6, gift from Jim Haseloff) to the C terminus of FEA2, with a 10-alanine spacer to improve stability and folding (Doyle and Botstein 1996). The C terminus of FEA2 was chosen because if the N terminus was extracellular, the low pH of the cell wall might inhibit GFP fluorescence (Scott et al. 1999). The FEA2–GFP fusion was driven by the 35S promoter in pRTL2 (Restrepo et al. 1990), and introduced into onion and *Arabidopsis* leaf epidermis by microprojectile bombardment.

Fluorescence from the FEA2–GFP fusion was observed using a confocal microscope, and was detected in a thin line at the cell periphery, consistent with plasma membrane localization (Fig. 7E–H) and similar to previous observations of GFP localization to the plasma membrane (Friedrichsen et al. 2000). The expression of free GFP also appeared at low magnification to be peripheral (Fig. 7A,D), due to the absence of GFP from the vacuole,
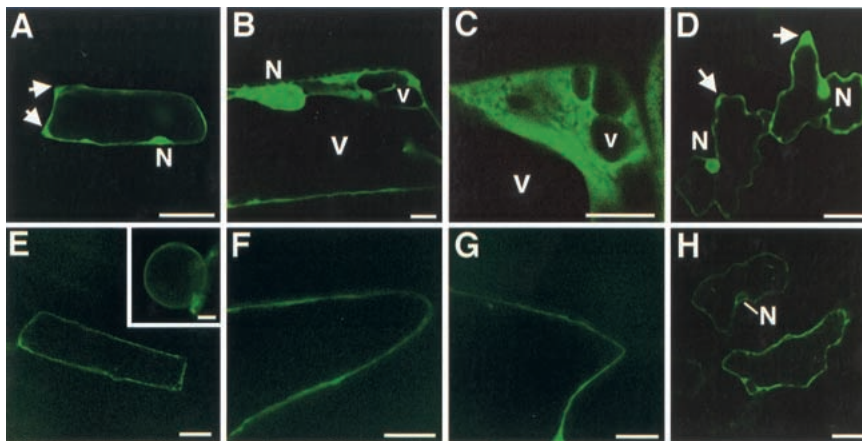

Figure 7. Subcellular localization of an FEA2–GFP fusion protein. Confocal microscopy images of cells expressing free GFP (*A–D*) or the FEA2–GFP fusion (*E–H*). *A–C* and *E–G* are images of onion scale epidermal cells. *D* and *H* are *Arabidopsis* leaf epidermal cells. In *A–D*, fluorescence is observed in cytoplasmic (arrowed) and nuclear (N) compartments, that are more easily visible at higher magnification in *B* and *C*. Most of the central region of each cell is occupied by the vacuoles (V), which do not accumulate the GFP. In *E–H*, FEA2–GFP fluorescence is visible in a narrow line in the position of the plasma-membrane, as well as in a perinuclear line in onion (*E*, inset) and *Arabidopsis* (N, panel *H*). In *A,E*, bar, 100 µm (10 µm in inset for panel *E*). In *B–D,F–H*, bar, 25 µm.

but at higher magnification the localization of free GFP throughout the cytoplasm and nucleoplasm was obvious (Fig. 7B,C). FEA2–GFP was also localized in a fine perinuclear line, possibly corresponding to the nuclear membrane (Fig. 7E inset, H). We also observed weak FEA2–GFP fluorescence in the cytoplasm in a reticulate pattern, similar to the pattern observed when cells express an endoplasmic reticulum (ER)-localized GFP (data not shown; Haseloff et al. 1997). We conclude that FEA2–GFP localizes in a pattern consistent with its targeting via the ER to the plasma membrane as well as to the nuclear membrane.

In conclusion, *fea2* mutants have massive overproliferation of the ear inflorescence meristem, and more modest effects on spikelet and floral meristems, floral organ number, and pedicel length. *fea2* encodes an LRR receptor-like protein that is expressed widely in immature shoot apical tissues and is a putative ortholog of *CLV2* from *Arabidopsis*. FEA2–GFP localizes to the plasma membrane, consistent with its proposed role as a receptor-like protein and suggesting that it interacts with an extracellular ligand to control stem cell proliferation in shoot meristems.

Discussion

fea2 is a novel mutant of maize that develops enlarged inflorescence and floral meristems. In each, the effect is qualitatively similar, therefore *fea2* normally functions in these meristems to restrict growth. However, *fea2* phenotypes range from a modest increase in organ number in ear spikelet pairs and in both male and female flowers, to a massive overproliferation of the ear inflorescence meristem. Furthermore, it is surprising that the tassel inflorescence meristem, which in early development is very similar to that of the ear (McSteen et al. 2000), is only mildly affected by *fea2* mutations, and does not develop strong fasciation. This difference could be explained by a redundant factor that can partially complement for *fea2* function in the tassel. Although *fea2* appears to be a single-copy gene in low stringency DNA blot hybridizations (data not shown), it is likely that there are multiple LRR receptor-like proteins, and cross talk between different LRR receptor-like or receptor proteins could account for genetic redundancy. Indeed, 30 CLV2-related LRR receptor-like proteins were found in the *Arabidopsis* genome sequence (Kaul et al. 2000). That the ear inflorescence meristem is more sensitive to loss of *fea2* function may be due to selection on the ear to form an enlarged structure, which can accommodate multiple rows of seed (Doebley 1992). The ear inflorescence apex may therefore have somewhat more relaxed constraints on meristem proliferation. This hypothesis is based on an assumption that ear inflorescence meristem size increased to produce more rows of seeds, an idea that is supported by biophysical models of phyllotaxy as well as by studies on the *abphyl1* mutation of maize that controls vegetative phyllotaxy (Green 1999; Jackson and Hake 1999). The difference between ear and tassel phenotypes might also be explained by the finding that the first products of the tassel inflorescence meristem are long branches that are initiated at about the same developmental stage as the inflorescence meristem starts to enlarge massively in *fea2* ears. Perhaps the generation of these long branch primordia in the *fea2* tassel depletes cells or growth potential from the inflorescence meristem at a critical stage when it would otherwise fasciate.

fea2 encodes an LRR receptor-like protein that is most similar to CLV2 from *Arabidopsis*. In fact, CLV2 is the only protein encoded in the *Arabidopsis* genome that has significant similarity to the non-LRR regions of FEA2, suggesting that these genes are orthologous. These findings prompt the question of how well the *CLV* pathway is conserved in maize. Biochemical and overexpression studies suggest that in *Arabidopsis*, CLV1 and CLV2 heterodimerize to form a receptor for the secreted CLV3 signaling protein (Brand et al. 2000; Trotochaud et al. 2000), though the involvement of CLV2 is not biochemically proven. If the *CLV* pathway is conserved, are the specificities of the hypothetical receptor–ligand and receptor–heterodimer interactions conserved? Some insights into these questions come from the comparison of FEA2 and CLV2 sequences.

The majority of FEA2 is made up of LRRs, motifs of around 24–29 amino acids that are commonly used for protein–protein interactions (Kobe and Deisenhofer 1994, 1995). FEA2 contains 19 LRRs, with an "island" of about 40 amino acids between LRR repeats 15 and 16. A similar island region separates the N-terminal LRRs from the four C-terminal LRRs in CLV2 (Jeong et al. 1999), the brassinosteroid receptor BRI1 (Li and Chory 1997), and the Cf resistance proteins of tomato (Thomas et al. 1997). Some insights into the control of receptor–ligand specificity have come from mutational and sequence analysis of these other LRR proteins. The LRR and transmembrane/juxtamembrane regions of BRI1 are sufficient for brassinosteroid perception, (He et al. 2000), and many *bri1* mutations are clustered in the island region and the first LRR after the island, suggesting that these regions are important for ligand specificity (Li and Chory 1997; Friedrichsen et al. 2000). However, in Cf4 and Cf9, tomato LRR receptor-like proteins for different fungal elicitors, the island regions are identical, and in these receptors the ligand specificity is likely determined by the N-terminal LRRs (Thomas et al. 1997; Wulff et al. 2001). Other studies of resistance genes also indicate that the LRRs confer specificity in ligand interaction (for reviews, see Ronald 1998; Martin 1999; Ellis et al. 2000; Richter and Ronald 2000). Therefore, the LRRs, and in the case of BRI1, the island region also, appear to be important for ligand binding specificity. It is intriguing that the island regions of FEA2 and CLV2 are poorly conserved. Either this region is not important for specificity, or, if it is, FEA2 and CLV2 may bind to unrelated ligands. There are, however, significant blocks of identity and similarity between FEA2 and CLV2 in the LRRs, some of which coincide to the predicted solvent-exposed residues involved in LRR–ligand interactions (Kobe and Deisenhofer 1995; Thomas et al. 1997). Therefore, if the LRRs of these proteins do indeed confer speci-

ficity, FEA2 and CLV2 could interact with related ligands.

Other features common in plant LRR proteins, including CLV2, include two pairs of cysteines spaced by six or seven amino acids that flank the LRRs, as well as a charged residue in the transmembrane region. These residues are proposed to mediate heterodimer formation (Jeong et al. 1999), and dimerization is a common feature for receptor activation, for example of receptor tyrosine kinases in animals (Ullrich and Schlessinger 1990; Schlessinger 2000). We do not know whether FEA2 forms a heterodimer in vivo, though it is likely because FEA2 has no obvious intracellular signaling domain. In contrast to CLV2, FEA2 has no charged residue in the transmembrane region, and lacks an N-terminal cysteine pair, but does have a C-terminal cysteine pair that is abnormally spaced by only four amino acids. Perhaps this is sufficient for dimerization of FEA2 with a hypothetical coreceptor. FEA2 also has several acidic residues in the extracellular region adjacent to the transmembrane domain that might also participate in a dimerization interface (Jeong et al. 1999).

In support of the hypothesis that monocots contain other components of the *CLV* pathway, a rice gene related to *CLV1*, *OsLRK1*, was recently isolated (Kim et al. 2000). *OsLRK1* antisense plants developed an increased number of various floral organs; however, meristem size was not measured. In addition, there was no obvious phenotypic effect of *OsLRK1* antisense expression in the inflorescence meristem, suggesting that this gene may be functionally distinct from *CLV1*. However, it is unclear whether the *OsLRK1* antisense plants represent a full loss of function. The isolation of null alleles would address this question, and help determine the extent of conservation of *CLV1* function in monocots.

fea2 is expressed widely in immature vegetative and inflorescence tissues, whereas it is down-regulated in expanded leaf tissue and is not expressed in the roots. The expression of *fea2* during vegetative development appears to have no functional significance, as we have not observed any phenotype of *fea2* mutants, for example in phyllotaxy or in leaf development. In addition to the inflorescence meristem phenotypes, *fea2* plants have an increase in floral organ number that is presumably a consequence of the enlarged floral meristems. Male flowers have an increase in stamen number, and female flowers have an increase in carpel number. *fea2* plants also have longer pedicels in the tassel spikelets, a phenotype that is reminiscent of the longer flower pedicel phenotype of *clv2* mutants (Kayes and Clark 1998). We did not measure spikelet pedicels in the ear because they are highly reduced. Although the pedicel phenotype has been interpreted as an organ development phenotype distinct from the meristem phenotypes of *clv2*, we prefer to interpret it as another class of meristem phenotype, because the pedicel is an internode, and internodes develop from meristematic cells marked by *KNOX* gene expression (Jackson et al. 1994). Mutations in the rice *OSH15 KNOX* gene, which is expressed in the intercalary meristem that forms the internode, are dwarf due to reduced internode elongation (Sato et al. 1999). Therefore, just as *fea2/CLV* and *KNOX* mutations have opposing phenotypes in the shoot apical meristem, they also have opposite effects on internode elongation.

FEA2 is predicted to be membrane localized, and visualization of FEA2–GFP is consistent with its targeting to the plasma membrane. We also observed fluorescence in the position of the nuclear membrane; the significance of this expression is unclear, though it was reproducible and occurred in cells that had only very weak FEA2–GFP fluorescence, so was not an artifact of very high overexpression. Whether the nuclear membrane localization is significant awaits independent confirmation, for example by immunolocalization. The apparent plasma membrane accumulation of FEA2–GFP supports the hypothesis that FEA2 acts as a receptor for an extracellular ligand. The subcellular localization of CLV2 has not been demonstrated, though according to its proposed function as a coreceptor with CLV1, it is also likely to be localized to the plasma membrane.

The fasciation phenotype of *fea2* mutants in the ear inflorescence meristem is much stronger than that described for *clv2* in *Arabidopsis* inflorescence meristems. By molecular and genetic criteria, *fea2-0* is likely a null allele. Similarly, the strong *clv2-1* allele is likely a null as it has a stop codon at amino acid 33 (Jeong et al. 1999). It appears that despite the segmental allotetraploid nature of the maize genome (Gaut and Doebley 1997), there is less functional redundancy for *fea2* in maize than for *CLV2* in *Arabidopsis*. Alternatively, unrelated genes or pathways may have been recruited to perform *CLV2*-related functions specifically in *Arabidopsis*. As already discussed, the ear inflorescence meristem may be sensitized to meristem enlargement due to prior selection for increased number of rows of seeds on the ear. During this selection, the teosinte inflorescence meristem, which initiates secondary meristems singly in a distichous phyllotaxy, was converted to the maize inflorescence meristem, which initiates multiple rows in a polystichous phyllotaxy (Beadle 1980; Doebley 1992). It is conceivable that the change in phyllotaxy during the selection for the maize ear was accompanied by an increase in inflorescence meristem size, possibly by modification of genetic pathways that regulate meristem size, such as the *CLV* pathway. An intriguing result in line with this hypothesis is that *fea2* maps to the location of a quantitative trait locus for seed row number, a measure of the number of vertical rows of seed on the ear (Veldboom and Lee 1994). Observing that *fea2* ears have up to twice the normal number of rows of seed, and that row number or spikelet density variants are of importance in other cereals such as barley, wheat, and rice (Futsuhara et al. 1979), it is possible that genes such as *fea2* could be manipulated to improve crop yields.

Materials and methods

Isolation of fea2

We initially identified a 4 kb *Sst*I *Mu8* hybridizing fragment that cosegregated with the *fea2-0* mutation, and through analysis of

lines with reduced *Mu* copy number found a corresponding 16-kb *Bam*HI fragment. Genomic DNA from *fea2* homozygous plants was digested with *Bam*HI and size-fractionated on a 0.8% agarose gel. DNA from several agarose strips in the 15–17 kb size range was extracted. After identification of the *Mu8*-containing fraction by Southern blotting, this DNA fraction was cloned into the λ dash vector (Stratagene), and the phage library was probed with a *Mu8* probe. Four positive clones were isolated and subclones were prepared for Southern blotting, sequencing and mapping; a 550-bp *Sst*I subclone was found to detect a polymorphism between DNA from *fea2-0* plants and normal sibs. To isolate the full-length coding sequence, cDNA was prepared from immature ear primordia of ~5–10 mm length using a reverse transcriptase kit (GIBCO BRL). Nested primers made to the 550-bp subclone sequence were used for 3′ RACE (Frohman et al. 1988) and amplified a product of ~1 kb that was cloned and sequenced. For isolation of the 5′ end of the coding sequence, a similar strategy was used, using cDNA prepared by the Marathon system (Clontech). The position of *Mu* insertions in the two *fea2* alleles was determined by sequencing of PCR products generated using a *Mu* end-specific primer and an *fea2*-specific primer. The *fea2* coding sequence was subsequently amplified by proofreading PCR (Extaq, Takara) from B73 genomic DNA and sequenced; this is the sequence shown in Figure 5. The sequence has been submitted to GenBank, accession no. AY055124.

RNA gel blot analysis

Maize tissues were ground to a fine powder in liquid nitrogen and RNA was isolated using the Trizol procedure, according to the manufacturer's instructions (GIBCO BRL). RNA concentrations were determined using a spectrophotometer, and equal loading was verified by ethidium bromide staining of the gel after electrophoresis. RNA was denatured and separated by electrophoresis according to the method of Smith et al. (1992). The RNA was transferred to a Hybond-N membrane (Amersham Pharmacia Biotech), and hybridization of ^{32}P-labeled probes was as described (Smith et al. 1992) at 42°C overnight. Blots were washed in 0.1× SSC, 0.1% SDS at 65°C for two times one h and exposed to a PhosphorImager screen (Fuji). For *fea2*, the 550-bp subclone downstream of the *Mu8* insertion site in *fea2-0* was used as a probe, and for *kn1* we used the whole cDNA (Vollbrecht et al. 1991).

Phenotypic analysis

All measurements were made on *fea2-0* mutants introgressed four or more generations into the B73 inbred background. B73 normal plants or heterozygous sibs were used as the control. Meristem measurements were made on fixed and cleared specimens, as described (Jackson and Hake 1999), and were made by defining the shoot meristem as the area of tissue distal to the most recently initiated primordium. Scanning electron microscopy was performed on fresh tissue using an S-3500N SEM (Hitachi). Samples were dissected and mounted on a stub in silver paint, and all cut tissue surfaces were sealed with silver paint (Electron Microscopy Sciences). Stubs were cooled on ice for 5–30 min before being transferred to the microscope. Imaging was performed at high vacuum using 3–5 kV accelerating voltage and a secondary electron detector. Images were collected electronically and transferred to Adobe Photoshop for generation of montages.

In situ hybridization

Maize ear primordia were dissected, vacuum infiltrated, and fixed in 4% formaldehyde, prepared fresh from paraformaldehyde (Sigma) in phosphate-buffered saline at 4°C overnight. In situ hybridizations were performed as described (Jackson et al. 1994).

FEA2–GFP imaging

PCR was used to generate a *Bam*HI restriction site to replace the stop codon of *fea2* and allow its fusion in-frame to a fragment comprising a 10-alanine linker followed by mGFP6 in pRTL2 (Restrepo et al. 1990). A 1300-bp PCR fragment was generated using a proofreading polymerase (ExTaq, Takara), and the primers 1b550-T7b CTTGATCTCTCCCGCAACGCCAT CTCC and *fea2*-3′Bam CTAGGATCCGCATATTCAACCCT CACAGGCC, and this fragment was cloned and then ligated together with the 5′ RACE PCR clone of *fea2* using a unique *Sbf*I site in the coding sequence. At the 5′ end, a *Xho*I site introduced when cloning the 5′ RACE product of *fea2*, 43 bp upstream of the ATG, was used to complete the cloning. The resulting construct contained the FEA2-alanine linker–GFP fusion under the control of a double 35S promoter. The part of the construct generated by the PCR was sequenced to check for possible amplification errors. Next, 0.5 µg of plasmid DNA from this construct, or a similar construct, pZY212, for expression of free GFP, was precipitated onto 1.5 mg of gold particles (1 µm, Biorad) according to the manufacturer's guidelines. The gold particles were resuspended in ethanol and divided into three aliquots for bombardments. Slices of onion scale or intact *Arabidopsis* plants that were grown under short day conditions for 4–5 wk were bombarded using a PDS-1000 system using 900 or 450 psi pressure, respectively. Bombarded samples were kept in the incubator for 2 d before observation of fluorescence spots with a Leica MZ FLIII fluorescence dissecting microscope and a Zeiss LSM confocal microscope. Images were scanned using a 20× objective or a 63× water immersion objective.

References

Barton, M.K. and Poethig, R.S. 1993. Formation of the shoot apical meristem in *Arabidopsis thaliana*—An analysis of development in the wild type and in the *shoot meristemless* mutant. *Development* **119:** 823–831.

Beadle, G.W. 1980. The ancestry of corn. *Sci. Am.* **242:** 112–119.

Birchler, J.A. 1993. Dosage analysis using B-A translocations. In *The maize handbook.* pp. 328–329. Springer Verlag, New York.

Bowman, J.L. and Eshed, I. 2000. Formation and maintenance of

the shoot apical meristem. *Trends Plant Sci.* **5:** 110–115.

Brand, U., Fletcher, J.C., Hobe, M., Meyerowitz, E.M., and Simon, R. 2000. Dependence of stem cell fate in *Arabidopsis* on a feedback loop regulated by CLV3 activity. *Science* **289:** 617–619.

Burr, B., Burr, F.A., Thompson, K.H., Albertson, M.C., and Stuber, C.W. 1988. Gene mapping with recombinant inbreds in maize. *Genetics* **118:** 519–526.

Clark, S.E., Running, M.P., and Meyerowitz, E.M. 1993. *CLAVATA1*, a regulator of meristem and flower development in *Arabidopsis*. *Development* **119:** 397–418.

———. 1995. CLAVATA3 is a specific regulator of shoot and floral meristem development affecting the same processes as CLAVATA1. *Development* **121:** 2057–2067.

Clark, S.E., Jacobsen, S.E., Levin, J.Z., and Meyerowitz, E.M. 1996. The *CLAVATA* and *SHOOT MERISTEMLESS* loci competitively regulate meristem activity in *Arabidopsis*. *Development* **122:** 1567–1575.

Clark, S.E., Williams, R.W., and Meyerowitz, E.M. 1997. The CLAVATA1 gene encodes a putative receptor kinase that controls shoot and floral meristem size in *Arabidopsis*. *Cell* **89:** 575–585.

Doebley, J. 1992. Mapping the genes that made maize. *Trends Genet.* **8:** 302–307.

Doyle, T. and Botstein, D. 1996. Movement of yeast cortical actin cytoskeleton visualized in vivo. *Proc. Natl. Acad. Sci.* **93:** 386–391.

Ellis, J., Dodds, P., and Pryor, T. 2000. Structure, function and evolution of plant disease resistance genes. *Curr. Opin. Plant Biol.* **3:** 278–284.

Emerson, R.A. 1912. Inheritance of certain "abnormalities" in maize. *Am. Breed. Assoc. Rept.* **8:** 385–399.

Endrizzi, K., Moussian, B., Haecker, A., Levin, J.Z., and Laux, T. 1996. The *SHOOT MERISTEMLESS* gene is required for maintenance of undifferentiated cells in *Arabidopsis* shoot and floral meristems and acts at a different regulatory level than the meristem genes *WUSCHEL* and *ZWILLE*. *Plant J.* **10:** 101–113.

Evans, M.M.S. and Barton, M.K. 1997. Genetics of angiosperm shoot apical meristem development. *Ann. Rev. Plant Physiol. Plant Mol. Biol.* **48:** 673–701.

Fletcher, L.C., Brand, U., Running, M.P., Simon, R., and Meyerowitz, E.M. 1999. Signaling of cell fate decisions by CLAVATA3 in *Arabidopsis* shoot meristems. *Science* **283:** 1911–1914.

Friedrichsen, D.M., Joazeiro, C.A.P., Li, J.M., Hunter, T., and Chory, J. 2000. Brassinosteroid-insensitive-1 is a ubiquitously expressed leucine-rich repeat receptor serine/threonine kinase. *Plant Physiol.* **123:** 1247–1255.

Frohman, M.A., Dush, M.K., and Martin, G.R. 1988. Rapid production of full-length cDNAs from rare transcripts: Amplification using a single gene-specific oligonucleotide primer. *Proc. Natl. Acad. Sci.* **85:** 8998–9002.

Futsuhara, Y., Kondo, S., and Kitano, H. 1979. Genetical studies on dense and lax panicles in rice. *Japan J. Breed* **29:** 239–247.

Gaut, B.S. and Doebley, J.F. 1997. DNA sequence evidence for the segmental allotetraploid origin of maize. *Proc. Natl. Acad. Sci.* **94:** 6809–6814.

Green, P.B. 1999. Expression of pattern in plants: Combining molecular and calculus based biophysical paradigms. *Am. J. Bot.* **8:** 1059–1076.

Hake, S. and Veit, B. 1988. New ear phenotype recovered in Mu field—"fascinated ear". *Maize Genet. Coop. Newslett.* **62:** 2.

Haseloff, J., Siemering, K.R., Prasher, D.C., and Hodge, S. 1997. Removal of a cryptic intron and subcellular localization of green fluorescent protein are required to mark transgenic

Arabidopsis plants brightly. *Proc. Natl. Acad. Sci.* **94:** 2122–2127.

He, Z.H., Wang, Z.Y., Li, J.M., Zhu, Q., Lamb, C., Ronald, P., and Chory, J. 2000. Perception of brassinosteroids by the extracellular domain of the receptor kinase BRI1. *Science* **288:** 2360–2363.

Jackson, D. and Hake, S. 1999. Control of phyllotaxy in maize by the *abphyl1* gene. *Development* **126:** 315–323.

Jackson, D., Veit, B., and Hake, S. 1994. Expression of maize *KNOTTED1* related homeobox genes in the shoot apical meristem predicts patterns of morphogenesis in the vegetative shoot. *Development* **120:** 405–413.

Jeong, S., Trotochaud, A.E., and Clark, S.E. 1999. The *Arabidopsis* CLAVATA2 gene encodes a receptor-like protein required for the stability of the CLAVATA1 receptor-like kinase. *Plant Cell* **11:** 1925–1933.

Kaul, S., Koo, H.L., Jenkins, J., Rizzo, M., Rooney, T., Tallon, L.J., Feldblyum, T., Nierman, W., Benito, M.I., Lin, X.Y., et al. 2000. Analysis of the genome sequence of the flowering plant *Arabidopsis thaliana*. *Nature* **408:** 796–815.

Kaya, H., Shibahara, K., Taoka, K., Iwabuchi, M., Stillman, B., and Araki, T. 2001. FASCIATA genes for chromatin assembly factor-1 in *Arabidopsis* maintain the cellular organization of apical meristems. *Cell* **104:** 131–142.

Kayes, J.M. and Clark, S.E. 1998. CLAVATA2, a regulator of meristem and organ development in *Arabidopsis*. *Development* **125:** 3843–3851.

Kellogg, E. and Birchler, J. 1993. Linking phylogeny and genetics: *Zea mays* as a tool for phylogenetic studies. *Syst. Biol.* **42:** 435–439.

Kerstetter, R.A., Laudencia-Chingcuanco, D., Smith, L.G., and Hake, S. 1997. Loss of function mutations in the maize homeobox gene, *knotted1*, are defective in shoot meristem maintenance. *Development* **124:** 3045–3054.

Kim, C.H., Jeong, D.H., and An, G.H. 2000. Molecular cloning and characterization of OsLRK1 encoding a putative receptor-like protein kinase from *Oryza sativa*. *Plant Sci.* **152:** 17–26.

Kobe, B. and Deisenhofer, J. 1994. The leucine-rich repeat—A versatile binding motif. *Trends Biochem. Sci.* **19:** 415–421.

———. 1995. A structural basis of the interactions between leucine-rich repeats and protein ligands. *Nature* **374:** 183–186.

Laufs, P., Dockx, J., Kronenberger, J., and Traas, J. 1998a. *MGOUN1* and *MGOUN2*: Two genes required for primordium initiation at the shoot apical and floral meristems in *Arabidopsis thaliana*. *Development* **125:** 1253–1260.

Laufs, P., Jonak, C., and Traas, J. 1998b. Cells and domains: Two views of the shoot meristem in *Arabidopsis*. *Plant Physiol. Biochem.* **36:** 33–45.

Laux, T., Mayer, K.F.X., Berger, J., and Jurgens, G. 1996. The *Wuschel* gene is required for shoot and floral meristem integrity in *Arabidopsis*. *Development* **122:** 87–96.

Leyser, H.M.O. and Furner, I.J. 1992. Characterisation of three shoot apical meristem mutants of *Arabidopsis thaliana*. *Development* **116:** 397–403.

Li, J.M. and Chory, J. 1997. A putative leucine-rich repeat receptor kinase involved in brassinosteroid signal transduction. *Cell* **90:** 929–938.

Long, J.A., Moan, E.I., Medford, J.I., and Barton, M.K. 1996. A member of the KNOTTED class of homeodomain proteins encoded by the SHOOTMERISTEMLESS gene of *Arabidopsis*. *Nature* **379:** 66–69.

Luckwill, L.C. 1943. The evolution of the cultivated tomato. *Jour. Royal Hort. Soc.* **68:** 19–25.

Martienssen, R. and Baron, A. 1994. Coordinate suppression of mutations caused by Robertson's Mutator transposons in

maize. *Genetics* **136:** 1157–1170.

Martin, G.B. 1999. Functional analysis of plant disease resistance genes and their downstream effectors. *Curr. Opin. Plant Biol.* **2:** 273–279.

Mayer, K.F., Schoof, H., Haecker, A., Lenhard, M., Jurgens, G., and Laux, T. 1998. Role of WUSCHEL in regulating stem cell fate in the *Arabidopsis* shoot meristem. *Cell* **95:** 805–815.

McSteen, I., Laudencia-Chingcuanco, I., and Colasanti, I. 2000. A floret by any other name: Control of meristem identity in maize. *Trends Plant Sci.* **5:** 61–66.

Medford, J. 1992. Vegetative apical meristems. *Plant Cell* **4:** 1029–1039.

Medford, J.I., Behringer, F.J., Callos, J.D., and Feldmann, K.A. 1992. Normal and abnormal development in the *Arabidopsis* vegetative shoot apex. *Plant Cell* **4:** 631–643.

Meyerowitz, E.M. 1997. Genetic control of cell division patterns in developing plants. *Cell* **88:** 299–308.

Muller, H.J. 1932. Further studies on the nature and causes of gene mutations. *Proc. Int. Congr. Genet.* **1:** 213–255.

Poethig, R.S. 1993. The maize shoot. In *The maize handbook*. pp. 11–16. Springer Verlag, New York.

Restrepo, M.A., Freed, D.D., and Carrington, J.C. 1990. Nuclear transport of plant potyviral proteins. *Plant Cell* **2:** 987–998.

Richter, T.E. and Ronald, P.C. 2000. The evolution of disease resistance genes. *Plant Mol. Biol.* **42:** 195–204.

Ronald, P.C. 1998. Resistance gene evolution. *Curr. Opin. Plant Biol.* **1:** 294–298.

Sato, Y., Sentoku, N., Miura, Y., Hirochika, H., Kitano, H., and Matsuoka, M. 1999. Loss-of-function mutations in the rice homeobox gene OSH15 affect the architecture of internodes resulting in dwarf plants. *EMBO J.* **18:** 992–1002.

Schlessinger, J. 2000. Cell signaling by receptor tyrosine kinases. *Cell* **103:** 211–225.

Scott, A., Wyatt, S., Tsou, P.L., Robertson, D., and Allen, N.S. 1999. Model system for plant cell biology: GFP imaging in living onion epidermal cells. *Biotechniques* **26:** 1125–1128.

Smith, L.G., Greene, B., Veit, B., and Hake, S. 1992. A dominant mutation in the maize homeobox gene, *Knotted-1*, causes its ectopic expression in leaf cells with altered fates. *Development* **116:** 21–30.

Sussex, I.M. 1952. Regeneration of the potato shoot apex. *Nature* **170:** 755–757.

Thomas, C.M., Jones, D.A., Parniske, M., Harrison, K., Balint-Kurti, P.J., Hatzixanthis, K., and Jones, J.D. 1997. Characterization of the tomato Cf-4 gene for resistance to Cladosporium fulvum identifies sequences that determine recognitional specificity in Cf-4 and Cf-9. *Plant Cell* **9:** 2209–2224.

Trotochaud, A.E., Hao, T., Wu, G., Yang, Z.B., and Clark, S.E. 1999. The CLAVATA1 receptor-like kinase requires CLAVATA3 for its assembly into a signaling complex that includes KAPP and a Rho-related protein. *Plant Cell* **11:** 393–405.

Trotochaud, A.E., Jeong, S., and Clark, S.E. 2000. CLAVATA3, a multimeric ligand for the CLAVATA1 receptor-kinase. *Science* **289:** 613–617.

Ullrich, A. and Schlessinger, J. 1990. Signal transduction by receptors with tyrosine kinase activity. *Cell* **61:** 203–212.

Veldboom, L.R. and Lee, M. 1994. Molecular-marker-facilitated studies of morphological traits in maize. 2. Determination of QTLs for grain-yield and yield components. *Theor. Appl. Genet.* **89:** 451–458.

Vollbrecht, E., Veit, B., Sinha, N., and Hake, S. 1991. The developmental gene *Knotted-1* is a member of a maize homeobox gene family. *Nature* **350:** 241–243.

Vollbrecht, E., Reiser, L., and Hake, S. 2000. Shoot meristem size is dependent on inbred background and presence of the

maize homeobox gene, knotted1. *Development* **127:** 3161–3172.

Weigel, D. and Clark, S.E. 1996. Sizing up the floral meristem. *Plant Physiol.* **112:** 5–10.

Wulff, B.B.H., Thomas, C.M., Smoker, M., Grant, M., and Jones, J.D.G. 2001. Domain swapping and gene shuffling identify sequences required for induction of an Avr-dependent hypersensitive response by the tomato Cf-4 and Cf-9 proteins. *Plant Cell* **13:** 255–272.

Zielinski, Q. 1945. Fascination in horticultural plants with special reference to the tomato. *Proc. Am. Hort. Sci.* **46:** 263–268.